

Anion Sensing Using Quinolinium Based Boronic Acid Probes

Ramachandram Badugu¹, Joseph R. Lakowicz*¹ and Chris D. Geddes*^{1,2}

¹Center for Fluorescence Spectroscopy, Department of Biochemistry and Molecular Biology, Medical Biotechnology Center, University of Maryland School of Medicine, 725 West Lombard St, Baltimore, MD, 21201, USA

²Institute of Fluorescence, Laboratory for Advanced Fluorescence Spectroscopy, Medical Biotechnology Center, University of Maryland Biotechnology Institute, 725 West Lombard St, Baltimore, MD, 21201, USA

Abstract: In this paper we review a series of water-soluble quinolinium boronic acid fluorescent probes, sensitive to halide and cyanide anions. We have intelligently combined the well-known halide, in particular chloride, bromide and iodide, sensing capability of the quinolinium nucleus with the fluoride or cyanide ion binding boronic acid moiety, to afford a range of water-soluble probes sensitive to fluoride, chloride, bromide, iodide and cyanide anions. These new probes offer the most attractive capability of sensing all important halides at physiological concentrations, coupled with a cyanide response at the lethal threshold level of about $\approx 20\text{-}30\ \mu\text{M}$. Some of the probes such as the BAQBAs show spectral shifts and intensity changes in the presence of fluoride and cyanide in a wavelength-ratiometric and colorimetric manner, enabling the detection of these anion concentrations at visible wavelengths. Although the sensing mechanism is different for fluoride and cyanide as compared to the other halides (chloride, bromide and iodide), the results reveal that these probes are in fact potential candidates towards the sensing of the all the halides and cyanide. Also we have constructed the corresponding control compounds that have no boronic acid moiety and are therefore insensitive to fluoride and cyanide but are mildly sensitive to chloride, bromide and iodide, similar to that of the boronic acid probes.

Keywords: Anion sensing, boronic acid based probes, stern-volmer equation, charge stabilization/neutralization, halides, cyanide, ratiometric sensing, lifetime based sensing, fluoride, chloride, bromide, iodide.

1. INTRODUCTION

The design and development of chemosensors for the detection of analytes, such as anions, cations, saccharides, etc., is an important topic of current research [1]. The reason for this interest is the importance of the detection and quantification of such analytes in disciplines such as the life sciences and environmental bio/chemistry. Among the anion sensors developed, those displaying an optical signal (transduction) are of special interest [2,3]. During the last few years we have made considerable progress in the development of anion fluorosensors for the detection of cyanide, halides, etc, using boronic acid containing fluorophores [4-9]. Subsequently in this review article we primarily focus our attention on the anion sensing ability of a few boronic acid probes developed recently in our laboratory, in contrast to their common role and application in glucose / monosaccharide determination [10-13].

The importance of halide detection and quantification can quite simply be judged by the vast amount of literature published over the last 20 or so years [14-18]. A clear summary on the halide abundance and the importance of each halide in analytical, environmental and physiological sciences is described in a recent review article [14]. Most biological fluids are complicated mixtures, which include

inorganic electrolytes such as halide ions. In plasma and muscle cells, electrolyte composition is normally fairly constant but in gastric/pancreatic juices, sweat, saliva and urine it may vary considerably, particularly when affected by illness. The elevated or reduced concentrations of each analyte might affect the normal body function. A good example of this is *Cystic fibrosis*, which is caused because of high concentration of chloride in patient's sweat or saliva as compared to that of non-cystic fibrosis patients. Fluoride is present in biological fluids and tissues and especially in bone and tooth. Fluoride is easily absorbed but is slowly excreted from the body, which can result in chronic poisoning, acute gastric and kidney disorders, dental and skeletal fluorosis and even death [14,15]. The physiological significance of the fluoride, chloride and iodide is well-known, but bromide is still considered either as a non-essential trace element or a trace element with an unknown function [19]. Iodine is however, unlike bromine an essential trace element in the human body [20]. The human body contains an average of 14 mg of iodine, concentrated mostly in the thyroid gland. Iodine containing hormones (thyroxin and triiodothyronine) strongly influence a range of biological reactions and iodine deficiency results in thyroid disease [20].

Cyanide is known as the sixth halide and is often termed *cyanogen*. The electronic structure and chemical properties of cyanide are very similar to that of the halogens. However, unlike the halides, cyanide is a notoriously toxic anion. The toxicity of its salts has been exploited for many hundreds of years. It was not until 1782 that cyanide itself was identified, isolated by the Swedish Chemist Scheele, who

*Address correspondence to this author at the Center for Fluorescence Spectroscopy, Department of Biochemistry and Molecular Biology, Medical Biotechnology Center, University of Maryland School of Medicine, 725 West Lombard St, Baltimore, MD, 21201, USA; E-mail: Geddes@umbl.umd.edu

later himself died from cyanide poisoning [21]. More recently cyanide was unsuccessfully used as a chemical warfare agent in World War I, primarily because of the way it was delivered [21], and is also thought to have been used against the inhabitants of the Kurdish city of Hama, Iraq [22], and in Shahabad, Iran, during the Iran-Iraq war [23]. Based on recent cyanide history, acute cyanide poisoning continues to constitute a threat for military forces in future conventional and unconventional conflicts [21].

Cyanide is also readily used in industry in the making of plastics, in the recovery of gold and silver from ores, and in the electroplating of metals, such as silver, gold, platinum and copper [21]. However, while cyanide is used in both military and industrial applications, cyanide poisoning is not common, but can more surprisingly occur from smoke inhalation from residential and industrial fires [21,24,25], where the combustion of synthetic products that contain carbon and nitrogen, such as plastics and synthetic fibers, release cyanide. Cigarette smoke also contains cyanide, the nonsmoker typically averages about 0.06 $\mu\text{g/mL}$ (2.31 μM) of cyanide in blood, where as a smoker typically averages 0.17 $\mu\text{g/mL}$ (6.5 μM) [26].

The mechanism of cyanide poisoning is by absorption, through the GI track, skin and lungs. Cyanide's toxicity lies in its ability to inhibit oxygen utilization by cells, binding to the active site of cytochrome oxidase [27,28], hence the tissues with the highest oxygen requirement (brain, heart and lungs) are the most affected by acute poisoning. There have been numerous studies of fire victims to assess the lethal levels of cyanide [21,24,25,29]. Fire survivors have been found to have < 20 μM cyanide in blood, while victims were found to have levels greater than = 20-30 μM and in some cases as much as 100 μM cyanide [21,29]. The estimated intravenous dose that is lethal to 50 % of the exposed population (LD_{50}) of HCN for a man is 1.0 mg/kg, and the estimated LD_{50} for liquid on the skin is about 100 mg/kg [21]. Hence any cyanide monitoring analytical technique would need a cyanide dynamic range from only few μM to < 30 μM to ensure physiological safeguard.

Numerous chemical and physicochemical methods for the detection and determination of cyanide, fluoride and the other halides such as potentiometric, chromatographic, spectrophotometric, flow injection and electrochemical analysis, to name but just a few, are available [30-54]. However, most of these systems are not cheap, portable and indeed field deployable, most requiring the benefits of an analytical laboratory [30-54].

It is well recognized that fluorescence techniques for sensing, such as lifetime, intensity and wavelength-ratiometric sensing [55,56] offer many advantages in the development of miniaturized, cheap, remote, accurate and

precise sensors for both laboratory and environmental sensing [55,56]. However, one constraint with fluorescence-based sensing to date, has been the development of suitable probes that show appropriate changes in their fluorescent properties at the required concentration range of a particular analyte, in the present case cyanide and halide anions.

Halides are known to be quenchers of common organic fluorophores [55]. Fluorescence quenching (quinine in dilute sulfuric acid by the addition of hydrochloric acid) was first reported in 1869 by George Stokes, and is now commonly attributed to the dynamic quenching by aqueous chloride ions [14]. Subsequently the quenching ability of the halides is widely utilized as a sensing mechanism, and many halide sensitive probes have subsequently been derived from quinine derivatives, which display a modest sensitivity for chloride due to their relatively long lifetimes when quaternised. While the un-protonated quinoline nucleus is only sparingly water soluble, its quaternised products are readily water-soluble and have subsequently been the transduction elements in many chloride/halide sensors [14].

It is not just the physiological significance of chloride that drives workers to mostly report the chloride sensitivity of some fluorescent probes, but because the quenching of fluorescence is not a selective process, and any fluorophore quenched by chloride is also quenched by bromide to a greater extent and also by iodide to an even greater extent. Therefore, for dynamic quenching, the sensitivity of fluorophores to halide is well known to be $\text{I}^- > \text{Br}^- > \text{Cl}^-$. The explanation of this effect lies in the fact that the efficiency of intersystem crossing to the excited triplet state, promoted by spin-orbit coupling of the excited singlet fluorophore and halide upon contact, depends on the mass of the quencher atom, hence the expression "heavy-atom effect" is sometimes used [14,55]. It is for this reason that the smallest-halide, fluoride, does not typically quench the fluorescence. As such, traditional halide sensitive probes are not very sensitive to fluoride and are therefore not suited for detecting fluoride < 50 mM [14]. Only a few fluorescent probes can be found in the literature which are sensitive to fluoride, all based on either the benzene or naphthalene backbone and therefore showing absorption in the deep UV (≈ 270 nm), which is not practical for many sensing applications [14,55,57]. Although water soluble sensor systems are deemed important, a few systems based on urea and thiourea based fluorophores were reported recently which show an optical response towards fluoride in organic media [58,59]. The new sets of probes described in this paper are readily water soluble and indeed show a selective fluoride response. Similar to fluoride, cyanide is not readily known as a dynamic quencher and hence most of the probes used for halide sensing are not sensitive to the cyanide anion.

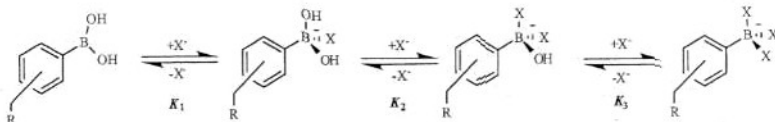


Fig. (1). Equilibrium involved in the interaction between the boronic acid group and fluoride or cyanide, where x denotes either cyanide or fluoride.

Table 1. Photophysical Data for BMQBAs^a, BMOQBAs^b, BAQBAs^c and Corresponding Control Compounds in Water at Room Temperature

	<i>o</i> -BMOQBA	<i>m</i> -BMOQBA	<i>p</i> -BMOQBA	BMQ
$\lambda_{\text{abs}}(\text{max}) / \text{nm}$	318, 346	318, 347	318, 346	318, 347
$\lambda_{\text{em}}(\text{max}) / \text{nm}$	450	450	451	453
ϕ_f	0.46	0.51	0.49	0.54
τ_f / ns	26.7	25.9	24.9	27.3
	<i>o</i> -BMQBA	<i>m</i> -BMQBA	<i>p</i> -BMQBA	BMQ
$\lambda_{\text{abs}}(\text{max}) / \text{nm}$	319	322	322	322
$\lambda_{\text{em}}(\text{max}) / \text{nm}$	427	427	427	427
ϕ_f	0.043	0.025	0.023	0.045
$\tau_f / \text{ns}^{\text{d}}$	4.01	3.72	2.10	2.59
	<i>o</i> -BAQBA	<i>m</i> -BAQBA	<i>p</i> -BAQBA	BAQ
$\lambda_{\text{abs}}(\text{max}) / \text{nm}$	381	381	398	391
$\lambda_{\text{em}}(\text{max}) / \text{nm}$	546	546	560	546
ϕ_f	0.04	0.038	0.036	0.041
$\tau_f / \text{ns}^{\text{d}}$	2.40	2.35	2.38	2.48

^{a,b,c}Adopted from references 12, 13 and 61 respectively. ^dMean fluorescence lifetime.

presented in (Table 1). Typical absorption and emission band maximum of the probes can be seen at 319 and 427 nm. The large Stokes-shifted fluorescence-emission band of ≈ 100 nm is ideal for fluorescence sensing, allowing easy discrimination of the excitation wavelengths [55]. All probes were found to be readily water soluble and have both modest quantum yields and lifetimes [12,13, 61].

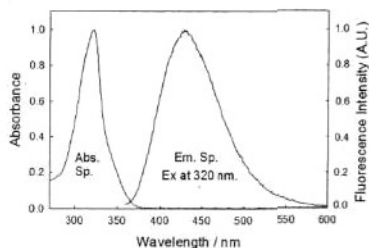


Fig. (4). Absorption and emission spectra of *o*-BMQBA in water. $\lambda_{\text{ex}} = 320$ nm. The spectra are representative of the respective isomeric phenylboronic acid containing fluorophores and the control compound.

Representative emission spectra of *o*-BMQBA in water with increasing concentrations of NaCl and the corresponding Stern-Volmer plots in water with three sodium halides are shown in (Fig. 5). BMQ and *m*- and *p*-BMQBAs show a very similar response towards the anions. The K_{SV} constants obtained using the relation $I/I_0 =$

$1 + K_{SV}[Q]$ for the control compound BMQ and BMQBAs are presented in (Table 2), where I and I_0 are the fluorescence intensity in the presence and absence of quencher, Q , respectively. As it can be seen from the figure about a 6-fold decrease is observed in *o*-BMQBA fluorescence intensity by the addition of 100 mM NaCl. The chloride response of all the probes is very similar (Table 2). Subsequently, these probes show a greater response in the presence of bromide and an even greater response to iodide due to the quenching ability order of the halides as discussed in the introduction. Accordingly, the fluorescence quenching mechanism is simply attributed to mostly halide collisional quenching. We also measured the lifetime for BMQ and the BMQBAs in water, in the presence of all three halides. The obtained K_{SV} data from the respective Stern-Volmer plots, is shown in (Table 2). The K_{SV} values obtained from lifetime measurements are smaller than that of intensity based measurements indicating a small but significant static quenching component of the probes by the halides. This behavior has previously been observed for quinolinium based probes [14]. Accordingly, BMQ and BMQBAs are potential candidates for the sensing of physiological chloride.

2.2. BMOQ and BMOQBA Probes

Fig. (6) shows the absorption and fluorescence emission spectra for *o*-BMOQBA in water. The other two isomers *m*- and *p*-BMOQBAs and the control compound BMQ show very similar spectral features. The photophysical data of BMQ and BMOQBAs is shown in (Table 1). Typical absorption and emission band maximum of the probes can be seen at 318 and 345 and 450 nm respectively for these

probes. The additional absorption band for these compounds at ≈ 350 nm compared to that of the BMQBA probes is attributed to the $n \rightarrow \pi^*$ transition of the oxygen [60]. The excitation independent emission band at ≈ 450 nm indicates only one ground-state species is present for both classes of probes. The large Stokes-shifted fluorescence emission band of ≈ 105 nm similar to the BMQBA probes is ideal for fluorescence sensing, allowing easy discrimination of the excitation wavelengths [55]. Additionally the relatively red-shifted absorption band of these compounds compared to that of the BMQ derivatives, has allowed us to use readily available cheap light sources for time-resolved measurements, such as LEDs. All probes were found to be readily water soluble. Unlike BMQ and the BMQBAs, BMOQ and the BMOQBAs have much higher quantum yields ≈ 0.5 , and much longer lifetimes of around 25 ns in water [12,13]. Interestingly, because of the longer lifetime of these probes, the quenching ability towards halides is expected to be more pronounced than the BMQBA probes. Subsequently, we tested the halide sensing ability of the BMOQ and BMOQBA probes in water, in the presence of halide. The representative emission spectra of *o*-BMOQBA in water with increasing concentrations of NaCl is shown in (Fig. 7). The fluorescence intensity of the probes decreases with increasing concentration of halides. (Fig. 7) also shows the corresponding Stern-Volmer plots obtained for *o*-BMOQBA in water with halide. The K_{SV} data for BMOQ and BMOQBAs is presented in (Table 2). The halide response of the other two isomers *m*-BMOQBA and *p*-BMOQBA and the control compound BMOQ is very similar to that of *o*-BMOQBA. As we can see, about a ≈ 9 -fold decrease in *o*-BMQBA fluorescence intensity is observed by the addition of 100 mM NaCl. As compared to the BMQ and the BMQBA probes, these probes show a more pronounced response (Table 2).

We also measured the lifetimes of BMOQ and the BMOQBAs in water, in the presence of halide, the obtained K_{SV} values shown in (Table 2). The K_{SV} values obtained from lifetime measurements are again relatively smaller than that of intensity based measurements, indicating a small but significant static fluorescence quenching component [14]. It is interesting to compare the halide sensing ability of the two sets of compounds discussed here. Because of the significantly long lifetime of the BMOQ and the BMOQBAs, then these probes are more sensitive to the halides.

2.3. BAQ and BAQBA Probes

After having successfully testing the halide sensing ability of the BMQ, and BMOQ series, discussed in sections 2.1 and 2.2, we moved our attention towards BAQ derivatives, (Fig 3). These derivatives are constructed using the stronger electron donating 6-amino substituent as compared to the 6-methyl or 6-methoxy substituent as in the BMQ or BMOQ classes of probes, respectively. Due to the new substituent, BAQ derivatives show unique spectral properties.

The absorption and emission spectra of these probes is considerably red-shifted, (Table 1). The typical absorption and emission band maximum of the probes are about 390

nm 565 nm, enabling the use of many light sources. The probes are readily soluble in water and show moderate quantum yields [61].

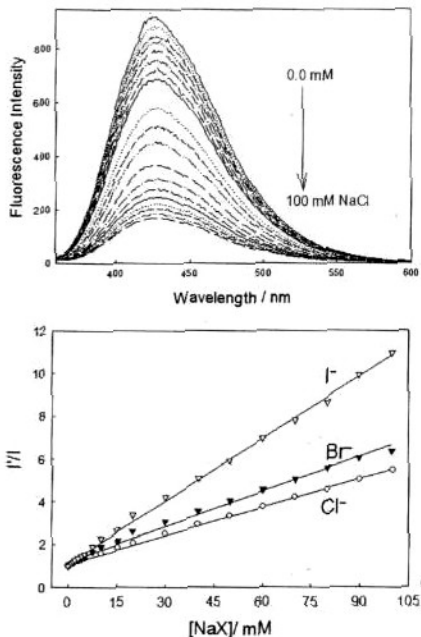


Fig. (5). Fluorescence emission spectra of *o*-BMOQBA in water with increasing concentrations of NaCl (top), $\lambda_{exc} = 320$ nm. The corresponding Stern-Volmer plots for *o*-BMOQBA with three halides (bottom).

Subsequently, we tested the response of BAQ and BAQBAs toward aqueous chloride, bromide and iodide. (Fig. 8) shows the fluorescence emission spectra of *o*-BAQBA in water with increasing concentrations of sodium iodide. The bottom panel of the figure shows the Stern-Volmer plots for *o*-BAQBA for all three halides in water. As expected, the steady-state Stern-Volmer constant for iodide was the largest, $K_{SV} = 34$ M⁻¹, with bromide and chloride very similar and substantially smaller than for iodide, 1.4 and 1.0 M⁻¹ respectively. A very similar response is observed for BAQ, and *m*- and *p*-BAQBAs in the presence of halide. The K_{SV} data for the probes is presented in (Table 2). We also measured the lifetime/s of BAQBA probes in the presence of halide to determine the dynamic quenching components. Interestingly the dynamic K_{SV} values were slightly smaller, $\approx 27, 0.4$ and 0.3 M⁻¹ for I⁻, Br⁻ and Cl⁻ respectively, suggesting a small, but measurable, static quenching component. A very similar finding that is noticed with other systems discussed in the previous sections.

Table 2. Stern-Volmer Constants (K_{SV} , M^{-1}) of the Probes Studied with Halides in Water^a

Probe	Cl ⁻		Br ⁻		I ⁻	
	Intensity	Lifetime	Intensity	Lifetime	Intensity	Lifetime
<i>o</i> -BMOQBA	170	97.3	332	237	471	364
<i>m</i> -BMOQBA	182	119	413	315	540	367
<i>p</i> -BMOQBA	177	111	370	231	595	331
BMOQ	222	152	384	363	520	425
<i>o</i> -BMQBA	44.0	22.2	55.0	32.6	97.0	48.1
<i>m</i> -BMQBA	20.0	12.3	32.0	20.1	48.0	26
<i>p</i> -BMQBA	17.0	11.8	26.5	12.5	42.0	25.9
BMQ	35.0	20.0	55.0	36.75	71.0	50.25
<i>o</i> -BAQBA	1.0	0.3	1.4	0.4	34.0	27.0
<i>m</i> -BAQBA	0.8	0.32	1.0	0.36	34.5	28.5
<i>p</i> -BAQBA	1.1	0.28	1.4	0.35	33.4	28.0
BAQ	1.0	0.3	1.5	0.42	33.0	27.5

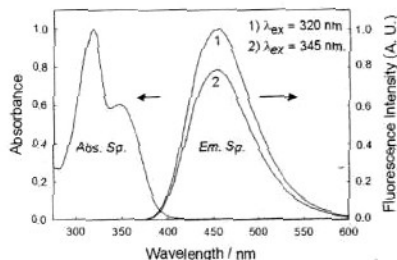
^aModified from reference 10.

Fig. (6). Absorption and emission spectra of *o*-BMOQBA in water. The spectra are representative of the respective isomeric phenylboronic acid containing fluorophores and the control compounds.

Our time-resolved studies have revealed that *o*-BAQBA is bi-exponential in Millipore water with lifetimes of 1.87 and 2.97 ns, with amplitudes of 0.52 and 0.48 respectively. Both the mean and amplitude weighted lifetimes were found to be 2.52 and 2.39 ns respectively. Interestingly, the lower response of BAQBA towards aqueous halide can be attributed to its reduced mean lifetime as compared to other quinolinium type fluorophores [14], noting the weak response towards aqueous Cl⁻, which could be particularly advantages when using BAQBA in physiological fluids for determining either aqueous fluoride or cyanide levels.

3. FLUORIDE AND CYANIDE SENSING

BMQ, BMOQ and BAQ, having no fluoride or cyanide binding boronic acid moiety, are insensitive towards these anions of interest. Accordingly, the spectral properties of these three probes are unaltered in the presence of fluoride or

cyanide. We give more comparative spectral evidence in this regard while discussing the response of the boronic acid probes towards fluoride or cyanide.

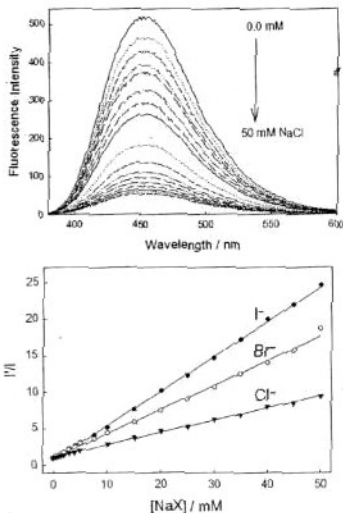


Fig. (7). Fluorescence emission spectra of *o*-BMOQBA in water with increasing concentrations of NaCl (top). λ_{ex} = 345 nm. The corresponding Stern-Volmer plots for *o*-BMOQBA in water with three sodium halides (bottom).

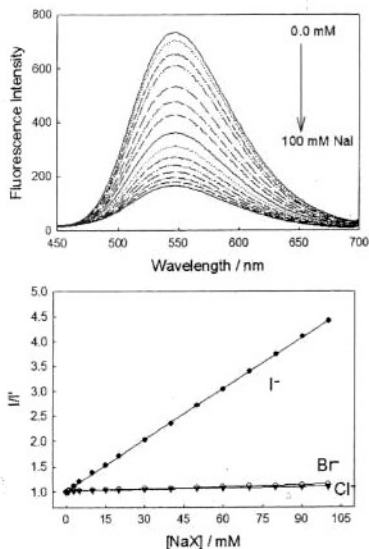


Fig. (8). A representative fluorescence emission spectra of *o*-BAQBA in water with increasing concentrations of NaI (top), $\lambda_{\text{ex}} = 358$ nm, and the corresponding Stern-Volmer plots with three sodium halides (bottom). A very similar response is observed for *m*-BAQBA and *p*-BAQBA with all three halides.

Table 3. Dissociation Constants of the Probes with Fluoride and Cyanide in Water

Probe	Fluoride (K_D / mM^3)	Cyanide (K_D / mM^3)
<i>o</i> -BMOQBA	960	52.9
<i>m</i> -BMOQBA	900	84.0
<i>p</i> -BMOQBA	1000	20.8
<i>o</i> -BMQBA	530	16.7
<i>m</i> -BMQBA	330	16.9
<i>p</i> -BMQBA	500	15.9
<i>o</i> -BAQBA	40.0	8.33
<i>m</i> -BAQBA	10.8	5.88
<i>p</i> -BAQBA	55.6	7.14

3.1. BMQBA Probes

3.1.1. Fluoride Sensing

The emission spectra of *o*-BMQBA in water with increasing concentrations of fluoride are shown in (Fig. 9). The other two isomers *m*- and *p*-BMQBA show a very

similar spectral response towards aqueous fluoride. The plots based on the normalized fluorescence intensity versus the fluoride concentration are shown in the bottom panel of (Fig. 9). The nonlinear response of the plots shown in the figure may be indicative of the complex binding interaction of fluoride with the boronic acid group. The calculated dissociation constants for all three probes with fluoride in water are shown in (Table 3). The corresponding control compound, not having a boronic acid group is non-responsive to fluoride.

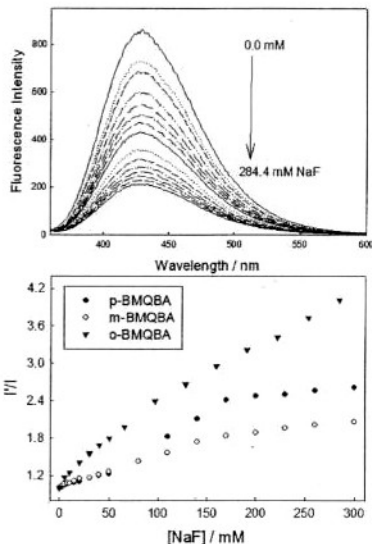


Fig. (9). Fluorescence emission spectra of *o*-BMQBA in water with increasing concentrations of NaF (top), $\lambda_{\text{ex}} = 320$ nm. The fluoride response plots of all three isomers (bottom).

3.1.2. Cyanide Sensing

Intensity Based Cyanide Sensing

(Fig. 10) shows the emission spectra for the *o*-BMQBA probe for increasing cyanide concentrations in water. All three isomeric boronic acid probes show a notable decrease in fluorescence intensity with μM cyanide concentrations [7]. BMQ is however relatively unperturbed, with a Stern-Volmer constant of $= 0.8 \text{ nM}^{-1}$. We again plotted the intensity ratiometric type plots for the data shown in (Fig. 10). (Fig. 10) shows an $= 13$ -fold decrease in fluorescence intensity with $30 \mu\text{M}$ cyanide for *m*-BMQBA, ideal for cyanide physiological safeguard monitoring. At the same sodium cyanide concentration the fluorescence intensity of *o*- and *p*-BMQBAs has reduced by factor of 9 and 7, respectively. Subsequently, all three probes saturate at about

40 μM NaCN, identifying the probes as potential candidates for cyanide detection at physiological safeguard levels [7].

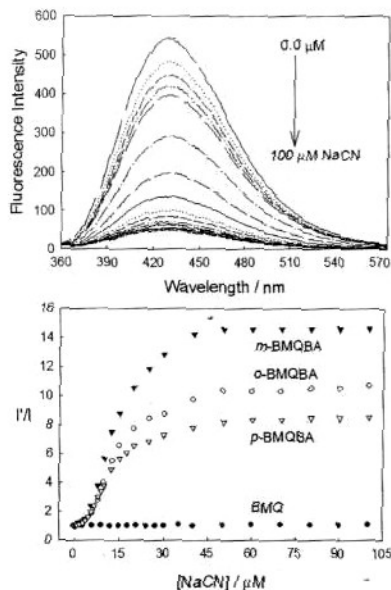


Fig. (10). Fluorescence emission spectra of *o*-BMOQBA in water with increasing concentrations of NaCN (top). $\lambda_{\text{ex}} = 320 \text{ nm}$. The cyanide response of all three isomers (bottom).

Table 4. Multiexponential Intensity Decay of BMQ and *o*-BMOQBA*

Compound	[CN ⁻] / μM	τ_1 (ns)	α_1	τ_2 (ns)	α_2	$\bar{\tau}$ (ns)	$\langle \tau^2 \rangle$ (ns)	χ^2
<i>o</i> -BMOQBA	0	2.18	0.4646	4.74	0.5354	4.01	3.55	1.00
	5	2.14	0.4615	4.45	0.5385	3.78	3.38	1.12
	10	2.28	0.5704	4.75	0.4296	3.78	3.34	1.04
	15	1.86	0.3265	3.64	0.6735	3.29	3.06	0.97
	20	1.88	0.3476	3.69	0.6524	3.30	3.06	1.04
	30	1.44	0.1762	3.27	0.8238	3.11	2.95	1.21
	40	1.92	0.3511	3.59	0.6489	3.21	3.00	0.90
BMQ	0	1.87	0.3320	3.58	0.6680	3.22	3.01	1.07
	0	2.59	1.0	---	---	2.59	2.59	1.07
	5	2.58	1.0	---	---	2.58	2.58	1.09
	10	2.59	1.0	---	---	2.59	2.59	1.07
	15	2.57	1.0	---	---	2.57	2.57	1.02
	20	2.57	1.0	---	---	2.57	2.57	1.12
	30	2.55	1.0	---	---	2.55	2.55	1.08
	40	2.55	1.0	---	---	2.55	2.55	1.14
	50	2.55	1.0	---	---	2.55	2.55	1.17

* $\lambda_{\text{ex}} = 372 \text{ nm}$, emission was collected with a 416 nm cut-off filter. BMQ $K_{12} = 314 \text{ M}^{-1}$. The free columns indicate that the intensity decay was not described well by the addition of an extra decay time, τ_2 .

Fluorescence Lifetime-based Cyanide Sensing

With notable changes in the fluorescence intensities of the probes in the presence of cyanide we questioned whether changes in the mean lifetime of the probe would also provide for lifetime based sensing. Our reasoning was based on the results obtained with 6-aminoquinolinium probes (BAQBAs), which show both spectral shifts and intensity changes in the presence of cyanide, allowing for both excitation and emission wavelength-ratiometric cyanide sensing (more in section 3.3) [4]. We have subsequently measured the lifetimes of the BMOQBA probes using the well-known Time-correlated Single Photon Timing Technique, TCSPC [4]. (Table 4) shows the intensity decay kinetics of BMQ and *o*-BMOQBA. The control compound BMQ was found to be mono-exponential in water with a lifetime of 2.59 ns. The presence of cyanide results in a slight decrease in the lifetime, the Stern-Volmer quenching constant $\approx 0.4 \text{ nM}^{-1}$, not unlike that determined from the intensity plots. The intensity decay of *o*-BMOQBA was found to be bi-exponential in water, with the mean lifetime decreasing from 4.01 to 3.22 ns in the presence of 50 μM cyanide, a $\approx 25\%$ change in mean lifetime which can not be explained by dynamic cyanide quenching, and is therefore attributed to the lifetime of the cyanide bound form.

3.2. BMOQBA Probes

3.2.1. Fluoride Sensing

(Fig. 11) shows the fluorescence emission spectra of *o*-BMOQBA in water with increasing concentrations of fluoride, the bottom panel of the figure representing the fluoride response of the three isomeric BMOQBAs. As shown here in (Fig. 11)-bottom, the other two isomers *m*- and *p*-BMOQBA show very similar spectral responses towards aqueous fluoride. The response plots were again fitted to the fluoride binding isotherm yielding the dissociation constants in the range 900-1000 mM^3 (Table 3). The BMOQBAs

discussed in the last section, show relatively lower K_D values as compared to the corresponding BMOQBAs. The control compound BMOQ, again having no boronic acid group, is non-responsive to the fluoride anion.

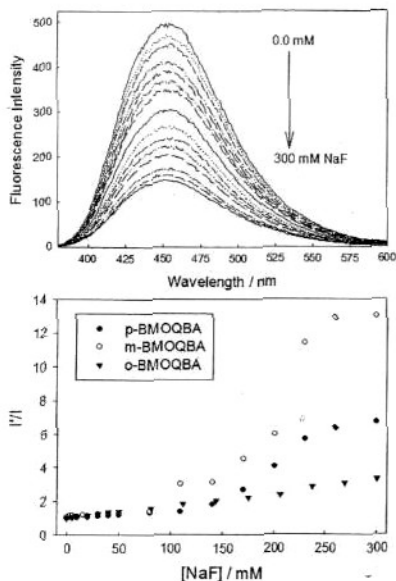


Fig. (11). Fluorescence emission spectra of *o*-BMOQBA in water with increasing concentrations of NaF (top). $\lambda_{ex} = 345$ nm. The fluoride response of all three isomers (bottom).

3.2.2. Cyanide Sensing

Intensity Based Cyanide Sensing

(Fig. 12) shows the emission spectra of *o*-BMOQBA in water for increasing cyanide concentrations, with $\lambda_{ex} = 345$ nm. As the cyanide concentration increases, the emission band at 450 nm decreases. For the control compound, BMOQ, we typically observed only a very slight decrease in emission intensity for increasing cyanide concentrations, which we have attributed to the dynamic fluorescence quenching by cyanide, noting that BMOQ does not possess a boronic acid group and therefore can not bind cyanide as postulated in our recent reports [4,5,7]. By plotting the intensity of BMOQ in the presence of cyanide, normalized by the intensity in the absence of cyanide, we were subsequently able to determine the Stern-Volmer quenching constant to be $\approx 3 \text{ nM}^{-1}$.

For the data shown in (Fig.12)-top, again we were able to construct intensity ratiometric type plots, i.e. the intensity in the absence of cyanide divided by the intensity in the presence of cyanide, (Fig. 12)-bottom. Interestingly the *m*-BMOQBA isomer shows a much stronger response to

cyanide with a 10-fold intensity change with as little as 20 μM cyanide. Similar to results obtained with BMOQBAs we were able to determine the cyanide dissociation constants for the *ortho*, *meta* and *para* boronic acid probes to be 52.9, 84.0 and 20.8 μM^3 , (Table 3), noting the units μM^3 or $\text{mol}^3 \text{ dm}^{-9}$ based on the equilibrium shown in (Fig. 1). These responses are most encouraging and suggest the use of these isomers for physiological cyanide safeguard. In addition, *m*-BMOQBA may find applications for cyanide determination post-mortem for fire victims, where cyanide levels exceed the $\approx 20 \mu\text{M}$ lethal concentration threshold [21].

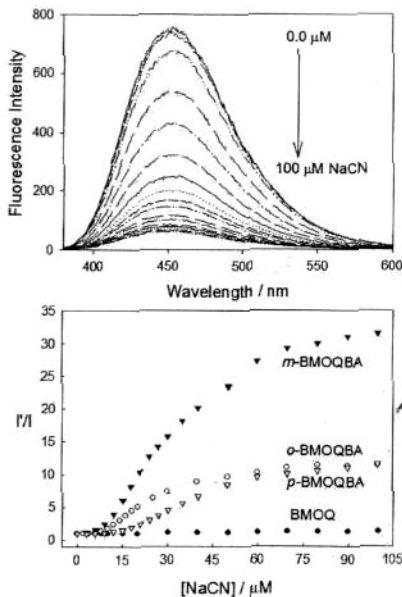


Fig. (12). Fluorescence emission spectra of *o*-BMOQBA in water with increasing concentrations of NaCN (top). $\lambda_{ex} = 345$ nm. The cyanide response of all three isomers (bottom).

To understand the different responses of the isomers towards cyanide it is informative to consider the charge neutralization-stabilization mechanism of these probes described in the (Fig. 2). Upon binding, the electron density on the boron atom of the probe is increased facilitating the partial neutralization of the positively charged quaternary nitrogen of the quinolinium moiety. The quaternary nitrogen not only reduces the pK_a of the probe [10-13], but also stabilizes the boronate-cyanide complex formed upon cyanide addition. The differences in cyanide sensitivity between the isomers is explained by either their through-space or through-bound interactions with the positively charged nitrogen, the *meta* form of the probes thought to interact via both mechanisms [4-7].

Table 5. Multiexponential Intensity Decay of BMOQ and *o*-BMOQBA^a

Compound	[CN ⁻] / μM	t_1 (ns)	α_1	τ_2 (ns)	α_2	$\bar{\tau}$ (ns)	$\langle \tau \rangle$ (ns)	χ^2
<i>o</i> -BMOQBA	0	26.71	1.0	---	---	26.71	26.71	1.33
	5	26.33	1.0	---	---	26.33	26.33	1.13
	10	26.34	1.0	---	---	26.34	26.34	1.21
	15	26.19	1.0	---	---	26.19	26.19	1.30
	25	24.78	1.0	---	---	24.78	24.78	1.23
	35	0.324	0.0160	25.54	0.9840	25.53	25.14	1.35
	45	0.326	0.0184	25.10	0.9816	25.09	24.64	1.46
	50	0.455	0.0176	25.20	0.9824	25.19	24.76	1.41
BMOQ	0	27.30	1.0	---	---	27.30	27.30	1.08
	5	27.04	1.0	---	---	27.04	27.04	1.10
	10	26.74	1.0	---	---	26.74	26.74	1.12
	15	26.53	1.0	---	---	26.53	26.53	1.06
	20	26.25	1.0	---	---	26.25	26.25	1.14
	30	25.86	1.0	---	---	25.86	25.86	1.17
	40	25.37	1.0	---	---	25.37	25.37	1.05
	50	25.00	1.0	---	---	25.00	25.00	1.16

^a $\lambda_{\text{ex}} = 372$ nm, emission was collected with a 416 nm cut-off filter. BMOQ $K_{\text{SF}} = 1840$ M⁻¹. The free columns indicate that the intensity decay was not described well by the addition of an extra decay time, τ_2 .

The dissociation constant values for *o*-BMQBA and *o*-BMOQBA are 16.7 and 52.9 mM³, respectively. Subsequently, this difference in the cyanide sensing ability of the *o*-BMQBA and *o*-BMOQBA is explained similarly to that described in the last paragraph. The relatively strong donating substituent $-\text{OCH}_3$ reduces the positive charge density on the quinolinium nitrogen center more effectively than the $-\text{CH}_3$ group does. Accordingly, BMQBAs with a

more positively charged nitrogen center, stabilize the anionic $[-\text{B}(\cdot)\text{X}_3]$ formed upon binding cyanide, yielding the lowered K_{D} values for the BMQBAs.

Fluorescence Lifetime-based Cyanide Sensing

The lifetime of *o*-BMOQBA was found to be monoexponential in water with a lifetime of 26.71 ns, (Table 5). However in the presence of cyanide the intensity

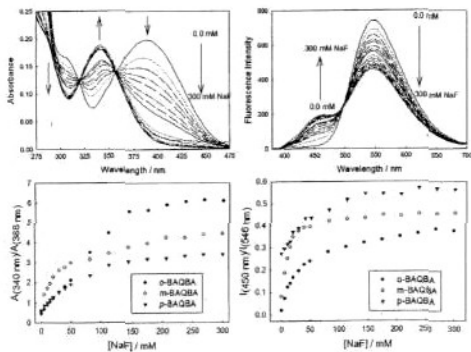


Fig. (13). Fluorescence absorption (top left) and emission (top right) spectra of *o*-BAQBA in water with increasing concentrations of NaF. $\lambda_{\text{ex}} = 358$ nm. The excitation (bottom left) and emission (bottom right) ratiometric plots for all three BAQBAs with fluoride.

of fluoride is biexponential with a much shorter component now present, ≈ 300 -450 ps. This has the result of reducing the mean lifetime by 4-8 % over the range of physiological cyanide importance. Interestingly these measurements were undertaken with a pulsed UV LED with an emission centered at 372 nm, suggesting the utility of the new probes for potential use in low power, field-deployable poison safeguard devices. Similar findings were observed for the other isomers.

The lifetime of the control compound BMOQ is monoexponential both in water and in the presence of cyanide, decreasing from 27.30 \rightarrow 25.0 ns with up to 50 μ M cyanide. In comparison, the lifetime of *o*-BMOQBA in water was found to be slightly shorter, 26.71 ns. We calculated the dynamic Stern-Volmer constant to be ≈ 2 nM⁻¹, which is very similar to the value obtained from the intensity-based measurements. Interestingly the presence of a much shorter lifetime component for *o*-BMOQBA with cyanide, suggests more than a simple collisional quenching process is present. Given this, and the fact that the intensity rapidly decreases in the presence of cyanide, we speculate that the cyanide bound probe has both a short lifetime, and a significantly reduced quantum yield as compared to the unbound probe form [7].

The BMOQBA's typically display a greater dynamic range for sensing, with notable changes observed in the cyanide concentration range 5 - 60 μ M. The BMOQBA's are highly water-soluble and can be prepared in a one step synthesis [13]. The ≈ 350 nm absorption band readily allows for UV LED excitation or even 370 / 400 nm laser diode excitation, which would not be possible with the BMOQBA's. The long lifetime of the BMOQBA's (≈ 26 ns) accounts for the cyanide collisional quenching, also observed with the control compound BMOQ. Subsequently, these probes are likely to be susceptible to other interferences such as aqueous chloride or oxygen [14,55].

The BMOQBA probes also show notable changes in fluorescence intensity in the presence of 30 μ M cyanide, 14 to 8-fold, for the *ortho* \rightarrow *para* isomers respectively. Unlike the BMOQBA probes, this class of probes shows a biexponential lifetime in water, and a relatively much shorter mean lifetime (4.01 ns) that decreases 25 % with the addition of 50 μ M cyanide. The lifetime reduction is thought to be due to the cyanide bound form, given the very minor changes observed with the control compound BMOQ. Interestingly, these probes are not likely to be perturbed much by other collisional quenchers due to their short lifetimes. With regard to fluorescence lifetime sensing, these changes are readily detectable using simple and cheap instrumentation [55]. One particular disadvantage of these probes however, is their requirement for UV excitation at 320 nm, which while possible with LEDs as shown here, limits their practical use in rapid analysis, portable, field deployable devices, areas of active research [55,62].

3.3 BAQBA Probes

3.3.1. Fluoride Sensing

Fig. 13) shows the absorption and emission spectra of *o*-BAQBA in Millipore water with increasing concentrations

of fluoride. As the concentration of fluoride increases, the absorption band at ≈ 388 nm decreases while the band at ≈ 342 nm increases. We can also see a significant change in the 388 nm band with each 5 mM fluoride increment. A similar response with fluoride is observed for *meta*- and *para*-BAQBA's. Subsequently, (Fig. 13) -bottom left shows the absorption wavelength ratiometric plot of the 342 and 388 nm bands for all three BAQBA's with fluoride. A linear response to fluoride was typically observed up to about 100 mM fluoride. As can be seen, the dynamic range for fluoride sensing is impressive where a ≈ 6 -fold change in A_{342}/A_{388} occurs up to ≈ 200 mM fluoride for *o*-BAQBA.

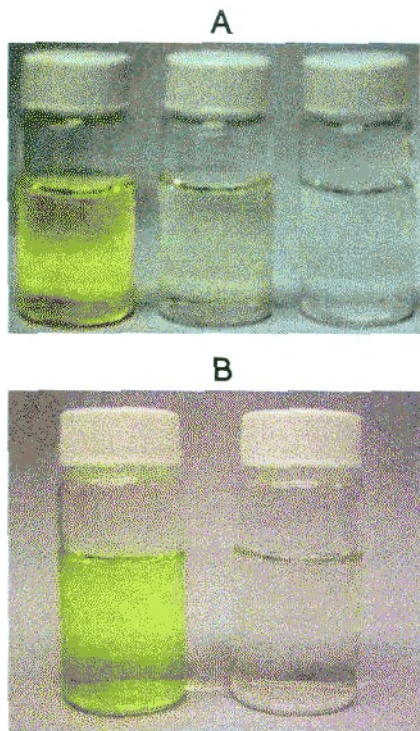


Fig. (14). (A) Photograph of three vials containing equal concentrations of *o*-BAQBA and 0, 50 and 300 mM fluoride, left to right respectively (B) A photograph of two vials containing equal amounts of *o*-BAQBA in water with 0 and 10 mM sodium cyanide, left and right respectively.

The fluorescence emission of *o*-BAQBA shows similar behavior ($\lambda_{ex} = 358$ nm) (Fig. 13)-top right, where the intensity of the band at 546 nm decreases while the emission band at 450 nm increases, noting the visible emission of the fluoride complexed form at 450 nm as compared to the red-

shifted emission of the uncomplexed form at 546 nm. This colorimetric response can also be seen visually as shown in (Fig. 14) where the three vials containing equal amounts of *o*-BAQBA in water with 0, 50 and 300 mM fluoride; the vial having no fluoride exhibits a greenish-yellow color and becomes slightly clear by adding 50 mM fluoride and eventually becomes completely colorless by the addition of 300 mM fluoride. For the data shown in (Fig. 13) - top right, we constructed the fluorescence emission ratiometric response, (Fig. 13) - bottom right. Again we were able to determine the dissociation constants of the probes with fluoride, (Table 3). Interestingly, the ratiometric response plots, (Fig 13)-bottom panels, show different dynamic sensing ranges, reflecting the differences in extinction coefficients and quantum yields of the F⁻ unbound and bound forms respectively.

We measured the lifetimes of *o*-BAQBA separately through two long pass filters, 416 and 546 nm, to investigate the lifetime changes during fluoride complexation. (Table 6) shows that the lifetime of the

uncomplexed fluoride probe form, i.e. visualized using the 546 nm long pass filter, remains biexponential upon fluoride addition, where the mean lifetime changes from 2.52 → 2.32 ns by the addition of 300 mM NaF. However, when we consider the lifetime of both bound and unbound forms using the 416 nm long pass filter, we find the intensity decay data is best described by a 3-exponential function with a short component now evident, which increases in amplitude (α_1) as the concentration of fluoride is increased. This short component, < 200 ps, is attributed to the fluoride bound form, shown after 358 nm steady-state illumination at 450 nm in (Fig. 13). As expected the amplitude weighted lifetime changes notably, from 2.41 → 1.84 ns, an = 25 % change. This suggests the possibility of lifetime based fluoride sensing using these new fluorescent probes. Similar results were found for all three BAQBA probes.

3.3.2. Cyanide Sensing

Very similar to that observed with fluoride, all three isomers show an excitation and emission wavelength-ratiometric response towards the cyanide anion. A

Table 6. Multiexponential Intensity decay of BAQ and *o*-BAQBA

Compound	[Fluoride] / μM	τ_1 (ns)	α_1	τ_2 (ns)	α_2	τ_3 (ns)	α_3	$\bar{\tau}$	$\langle \tau \rangle$	χ^2
BAQ	0	2.48	1	-	-	-	-	2.48	2.48	1.10
	(416 nm) ^a									
	0b	1.99	0.675	3.28	0.325	-	-	2.36	2.41	1.01
	30b	1.27	0.230	2.58	0.770	-	-	2.41	2.28	1.26
	60	0.14	0.110	1.99	0.700	3.96	0.190	2.66	2.16	0.97
	90	0.18	0.120	1.80	0.510	3.01	0.370	2.44	2.05	1.06
	120	0.17	0.150	1.83	0.530	3.06	0.320	2.42	1.97	1.15
	150	0.14	0.150	1.56	0.380	2.81	0.470	2.39	1.93	0.95
	200	0.18	0.180	1.85	0.590	3.33	0.230	2.42	1.89	0.98
	250	0.18	0.200	1.83	0.610	3.59	0.190	2.45	1.83	1.06
	300	0.22	0.210	1.92	0.670	4.19	0.120	2.49	1.84	1.24
<i>o</i> -BAQBA	(546 nm) ^b									
	0	2.00	0.620	3.07	0.380	-	-	2.52	2.41	0.89
	30	1.86	0.540	2.89	0.460	-	-	2.45	2.33	0.90
	60	1.93	0.720	3.41	0.280	-	-	2.53	2.34	0.95
	90	1.67	0.420	2.73	0.580	-	-	2.40	2.28	1.08
	120	1.70	0.510	2.89	0.490	-	-	2.44	2.28	1.15
	150	1.73	0.580	2.99	0.420	-	-	2.43	2.26	1.02
	200	1.54	0.410	2.67	0.590	-	-	2.35	2.21	1.04
	250	1.57	0.500	2.78	0.500	-	-	2.34	2.18	1.00
	300	1.59	0.520	2.77	0.480	-	-	2.32	2.16	1.10

^aLong pass filters; ^bNo notable improvement in fit could be obtained using a 3-exp function. Similar values were also found for the *meta*- and *para*-BAQBA probes.

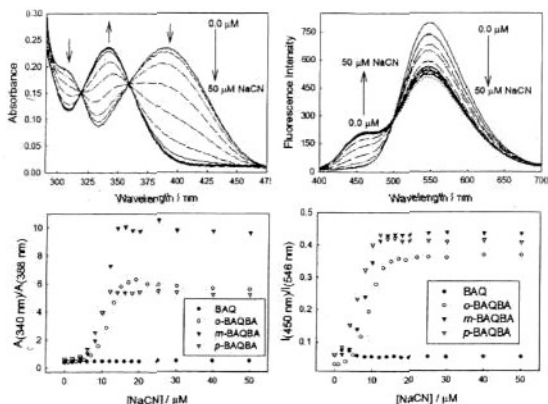


Fig. (15). Fluorescence absorption (top left) and emission (top right) spectra of *o*-BAQBA in water with increasing concentrations of NaCN. $\lambda_{ex} = 358$ nm. The excitation (bottom left) and emission (bottom right) wavelength-ratiometric plots for all three BAQBAs with cyanide.

representative absorption and emission spectra of *o*-BAQBA in water with increasing concentrations of cyanide and the corresponding wavelength-ratiometric plots obtained with A_{388}/A_{345} nm and I_{566}/I_{450} nm are shown in (Fig. 15). For comparison the ratiometric plot of the control compound is also included in (Fig. 15). The absorption or fluorescence spectra of BAQ are unchanged by the addition of the cyanide. However, all three boronic acid probes show similar response to cyanide. Interestingly, *m*-BAQBA shows a relatively much stronger response with a greater dynamic sensing range than *o*-BAQBA and *p*-BAQBA, (Fig. 15)-bottom panel. By comparing (Fig. 15)-bottom right and left, we can see that a greater change is observed for the ratiometric absorption measurements, reflecting the difference in the extinction coefficient and the quantum yields of the cyanide unbound and bound forms, respectively. The dissociation constants calculated from the plots for *o*-, *m*- and *p*-BAQBAs are 8.33, 5.88 and 7.14 μM^2 , respectively (Table 3). The probes saturate below 20 μM cyanide, suggesting the probes as potential candidates to monitor lethal cyanide levels.

The BAQBA probes also show a colorimetric-type response to cyanide as shown in (Fig. 14). The two vials contain equal concentrations of *o*-BAQBA, with both zero and 10 μM NaCN respectively. It can be readily seen from the figure that the color change can be easily visualized, suggesting the use of these BAQBA probes for simple colorimetric cyanide determination.

The dual emission bands have enabled us to clearly resolve the lifetime of both the cyanide bound and unbound probe forms where we concluded that the bound form had a much shorter lifetime, a few hundred ps, in comparison to the unbound form which had a mean lifetime of 2.59 ns. The detailed time-resolved data for *o*-BAQBA and BAQ in water with cyanide has been recently reported by us [4].

4. CONCLUSIONS

In this review article we have demonstrated a rationale for constructing new anion probes based on two different transduction mechanisms of sensing. These new probes are unique in that they couple both the halide quenching ability of the quinolinium nucleus, with the ability to chelate both cyanide and fluoride, which can't otherwise be readily sensed by other fluorescence means. The new probes are readily water-soluble, have high quantum yields and have the dynamic sensing ranges main stream within the concentration ranges of both physiological and industrial importance. To some degree, these ranges are also somewhat tunable.

ACKNOWLEDGEMENTS

This work was supported by the NIH, USA, National Center for Research Resources, RR-08119. Partial salary support to JRL from UMBI is also gratefully acknowledged.

ACRONYMS AND SYMBOLS

BAQ	= <i>N</i> -(Benzyl)-6-aminoquinolinium bromide
BMQ	= <i>N</i> -(Benzyl)-6-methylquinolinium bromide
BMOQ	= <i>N</i> -(Benzyl)-6-methoxyquinolinium bromide
<i>o</i> -, <i>m</i> -, or <i>p</i> -BAQBA	= <i>N</i> -(2-, 3-, or 4-Boronobenzyl)-6-aminoquinolinium bromide
<i>o</i> -, <i>m</i> -, or <i>p</i> -BMQBA	= <i>N</i> -(2-, 3-, or 4-Boronobenzyl)-6-methylquinolinium bromide
<i>o</i> -, <i>m</i> -, or <i>p</i> -BMOQBA	= <i>N</i> -(2-, 3-, or 4-Boronobenzyl)-6-methoxyquinolinium bromide

- LED** = Light Emitting Diode
SPQ = *N*-(3-sulphopropyl)-6-methoxyquinolinium
TCSPC = Time-Related Single Photon Counting

REFERENCES

- [1] Martínez-Máñez, R.; Sancenón, F. *Chem. Rev.*, **2003**, *103*, 4419.
 [2] Gale, P.A. *Coord. Chem. Rev.*, **2001**, *213*, 79-128.
 [3] Gale, P.A. *Coord. Chem. Rev.*, **1999**, *199*, 181-233.
 [4] Badugu, R.; Lakowicz, J.R.; Geddes, C.D. *Anal. Biochem.*, **2004**, *327*, 82-90.
 [5] Badugu, R.; Lakowicz, J.R.; Geddes, C.D. *Dyes and Pigments*, **2005**, *64*(1), 49-55.
 [6] Badugu, R.; Lakowicz, J.R.; Geddes, C.D. *Sensors Actuators B: Chem.*, **2005**, *104*(1), 103-110.
 [7] Badugu, R.; Lakowicz, J.R.; Geddes, C.D. *Anal. Chim. Acta*, **2004**, *522*(1), 9-17.
 [8] Badugu, R.; Lakowicz, J.R.; Geddes, C.D. *J. Fluores.*, **2004**, *14*, 693-698.
 [9] Badugu, R.; Lakowicz, J.R.; Geddes, C.D. *J. Am. Chem. Soc.* In press.
 [10] Badugu, R.; Lakowicz, J.R.; Geddes, J. *Fluores.*, **2004**, *14*(5), 617-633.
 [11] Badugu, R.; Lakowicz, J.R.; Geddes, C.D. In *Reviews in Fluorescence 2005*; Geddes, C.D.; Lakowicz J.R. Eds; Kluwer/Plenum publishers: New York, **2005**, In press.
 [12] Badugu, R.; Lakowicz, J.R.; Geddes, C.D. *Talanta*, **2005**, *65*, 762-768.
 [13] Badugu, R.; Lakowicz, J.R.; Geddes, C.D. *Bioorg. Med. Chem.*, **2005**, *13*, 113-119.
 [14] Geddes, C.D. *Meas. Sci. Technol.*, **2001**, *12*, R53.
 [15] Kista, E. *Chin. Chem.*, **1987**, *33*, 253.
 [16] Michigami, Y.; Kurode, Y.; Ueda, K.; Yamamoto, K. *Anal. Chim. Acta*, **1993**, *274*, 299.
 [17] Seifert, K.; Dominik, B.; Dominik, G. W. *Fluoride*, **1986**, *19*, 22.
 [18] Tyler, J.E.; Poole, D.F.G. *Arch. Oral. Biol.*, **1989**, *34*, 995.
 [19] Buchberger, W.; Huebner, U. *Mikrochim. Acta*, **1989**, *3*, 137-142.
 [20] Prasad, A.S. Trace Elements and Iron in the Human Metabolism; Plenum: New York, **1978**.
 [21] Baskin, S.I.; Brewer, T.G. In *Medical Aspects of Chemical and Biological Warfare*, Sidell, F.; Takafuji, E.T.; Franz, D.R. Eds; TMM publications; Washington, **1997**, Chapter 10, p. 271-286 and references cited therein.
 [22] Lang, J.S.; Mullin, D.; Fenyvesi, C.; Rosenberg, R.; Barnes, J. *US News & World Report*, November 10, **1986**, 29.
 [23] Medical expert reports use of chemical weapons in Iran-Iraq war, *UN Chronicle* **22**, **1985**, 24-26.
 [24] Ishii, A.; Seno, H.; Watanabe-Suzuki, K.; Suzuki, O.; Kumazawa, T. *Anal. Chem.*, **1998**, *70*(22), 4873-4876.
 [25] Moriya, F.; Hashimoto, Y. *J. For. Sci.* **2001**, *46*(6), 1421-1425.
 [26] Clark, C.J.; Campbell, D.; Reid, W.H. *Lancet*, **1**, **1981**, 1332-1335.
 [27] Warburg, O.; Hoppe-Seyler's, Z. *Physiol. Chem.*, **1911**, *76*, 331-346.
 [28] Kellin, D. *Proc. R. Soc. Lond. B. Biol. Sci.* **1929**, *104*, 206-251.
 [29] Baud, F.J.; Barriot, P.; Toffis, V. *N. Engl. J. Med.*, **1991**, *325*, 1761-1766.
 [30] Giurati, C.; Cavalli, S.; Gorni, A.; Badocco, D.; Pastore, P. *J. Chromat. A*, **2004**, *1023*, 105-112.
 [31] Beck, H. P.; Zhang, B.; Bordeau, A. *Anal. Lett.*, **2003**, *36*, 2211-2228.
 [32] Fernandez-Arguelles, M.T.; Costa-Fernandez, J.M.C.; Pereiro, R.; Sanz-Medel, A. *Anal. Chim. Acta*, **2003**, *491*, 27-35.
 [33] Deep, B.; Balasubramanian, N.; Nagaraja, K. S. *Anal. Lett.*, **2003**, *36*, 2865-2874.
 [34] Favero, J.A.D.; Tubino, M. *Anal. Sci.*, **2003**, *19*, 1139-1143.
 [35] Ros-Lis, J.V.; Martínez-Manez, R.; Soto, J. *Chem. Commun.*, **2002**, 2248-2249.
 [36] Cho, K.; Jang, Y.S.; Gong, M.S.; Kim, K.; Joo, S.W. *Appl. Spectrosc.*, **2002**, *56*, 1147-1151.
 [37] Drochiolu, G. *Anal. Bioanal. Chem.*, **2002**, *372*, 744-747.
 [38] Hughes, C.; Lehner, F.; Dirikolu, L.; Harkins, D.; Boyles, J.; McDowell, K.; Tobin, T.; Crutchfield, J.; Sebastian, M.; Harrison L.; Baskin, S. I. *Toxicol. Mech. Methods*, **2003**, *13*, 129-138.
 [39] Ipatov, A.; Ivanov, M.; Makarychev-Mikhailov, S.; Kolodnikov, V.; Legin, A.; Vlasov, Y. *Talanta*, **2002**, *58*, 1071-1076.
 [40] Hashino, M.; Nagashina, K.; Kamaya, M. Nakano, N.; *Bunseki Kagaku*, **2003**, *52*, 481-484.
 [41] Drochiolu, G. *Talanta*, **2002**, *56*, 1163-1165.
 [42] Traçaqui, A.; Raul, J.S.; Gerau, A.; Berteloni, L.; Ludes, B. *J. Anal. Toxicol.*, **2002**, *26*, 144-148.
 [43] Vallejo-Pecharroman, B.; de Castro, M.D.L. *Analyst*, **2002**, *127*, 267-270.
 [44] Premasiri, W.R.; Clarke, R.H.; Lonthe, S.; Womble, M.E.; *J. Raman Spectrosc.*, **2001**, *32*, 919-922.
 [45] Barnes, D.E.; Wright, P.J.; Graham, S.M.; Jones-Watson, E.A. *Geostandards Newsletter-The Journal of Geostandards and Geoanalysis*, **2000**, *24*, 183-195.
 [46] Recalde-Ruiz, D. L.; Andres-Garcia, E.; Daiz-Garcia, M.E. *Analyst*, **2000**, *125*, 2100-2105.
 [47] Recalde-Ruiz, D.L.; Andres-Garcia, E.; Daiz-Garcia, M. E. *Quimica Anal.*, **1999**, *18*, 111-113.
 [48] Mansfeldt, T.; Biernath, H. *Anal. Chim. Acta*, **2000**, *406*, 283-288.
 [49] Nakamura E.; Yagi, M. *Bunseki Kagaku*, **2000**, *49*, 55-58.
 [50] Miralles, E.; Compano, R.; Granados, M.; Prat, M.D. *Anal. Chim. Acta*, **2000**, *403*, 197-204.
 [51] Frant, M.S.; Ross, J.W. *Science*, **1966**, *154*, 1553.
 [52] Culik, B. *Anal. Chim. Acta*, **1986**, *189*, 329.
 [53] Ikenishi, R.; Kitagawa, T. *Chem. Pharm. Bull.*, **1988**, *36*, 810.
 [54] Yamamoto, H.; Ori, A.; Ueda, K.; Dusemund, C.; Shinkai, S. *Chem. Commun.*, **1996**; (3): 407.
 [55] Lakowicz, J. R. *Principles of Fluorescence Spectroscopy*, 2nd Edition, Kluwer/Academic Plenum Publishers: New York, **1997**.
 [56] Gryczynski, Z.; Gryczynski, I.; Lakowicz, J.R. *Methods in Enzymology*, **2002**, *360*, 44-75.
 [57] Cooper, C.R.; Spencer, N.; James, T.D. *Chem. Commun.*, **1998**, 1365.
 [58] Jimenez, D.; Martínez-Manez, R.; Sancenón, F.; Soto, J. *Tet. Lett.*, **2002**, *43*, 2823-2825.
 [59] Cho, E.J.; Moon, J.W.; Ko, S.W.; Lee, J.Y.; Kim, S.K.; Yoon, J.; Nam, K.C. *J. Am. Chem. Soc.*, **2003**, *125*, 12376-12377.
 [60] Geddes, C.D. *Sensors Actuators B: Chem.*, **2001**, *72*, 188-195.
 [61] Badugu, R.; Lakowicz, J.R.; Geddes, C.D. *Talanta*, In press.
 [62] Landgraf, S. In *Reviews in Fluorescence 2004*; Geddes, C.D.; Lakowicz, J.R. Eds.; Springer publishers: New York, **2004**.